JPL PUBLICATION 77-66

Sampled Data Analysis of a Computer-Controlled Manipulator

National Aeronautics and Space Administration

Jet Propulsion Laboratory
California Institute of Technology
Pasadena, California 91103

JPL PUBLICATION 77-66

Sampled Data Analysis of a Computer-Controlled Manipulator

B. R. Markiewicz

October 15, 1977

National Aeronautics and
Space Administration

Jet Propulsion Laboratory
California Institute of Technology
Pasadena, California 91103

Prepared Under Contract No. NAS 7-100
National Aeronautics and Space Administration

PREFACE

The work described in this report was performed by the Guidance and Control Division of the Jet Propulsion Laboratory.

ABSTRACT

A comprehensive sampled data analysis of a computer-controlled manipulator is presented in terms of root loci for gain selection and transient responses to step input functions. All parameter values and their derivations where applicable are tabulated. The analysis, while quite specific, uses normalized gain parameters, which allows the results to be applied to any similar system regardless of individual hardware parameter values.

CONTENTS

Figures

Tables

SECTION I

INTRODUCTION

The JPL Robot Research Program has the goal of applying robotics to space exploration. As space mission requirements become more complex and communication delays become longer, spacecraft must have more autonomy to be able to perform useful tasks. Both these problems, complexity and communication delay, are present in planetary surface rovers. For example, a rover must coordinate the functions of manipulation, vision, and locomotion in order to carry out tasks of scientific interest. Furthermore, at earth-Mars distances, communication delays range from 8 to 40 min, limiting direct control to very simple tasks.

Since a planetary rover is an obvious candidate for robotic applications, the JPL Robot Research Program has developed a breadboard Mars roving vehicle. This breadboard development was chosen to give focus to the program, and also represents the problem of developing basic robotic capabilities (manipulation, vision, and locomotion) and coordinating their operation. Typical surface exploration tasks were selected, consisting of sample (rock, etc.) handling, and instrument assembly and deployment. Sample handling and assembly impose stringent requirements on manipulator motion. For sample handling, the manipulator must operate in an imprecisely known environment, avoiding obstacles which change at various times. During assembly tasks, the environment is fairly well known, but precise parts placement is important. Both of these tasks then impose requirements for precise control over the manipulator's motion: sample handling during the large motions and assembly at the motions' end points. Additionally, the desired space application necessitates a simple program, one which need not be run by a large computer. Meeting the precise control requirements requires a thorough knowledge of the control stability and transient response characteristics of the closed-loop feedback system. It is the intent of this report to present that information.

Since the primary purpose of the rover development was to build an overall rover system, subsystem technology was adapted from existing designs wherever possible. The JPL rover manipulator design was based on work originally done at Stanford University's Artificial Intelligence Laboratory. Since JPL's requirements differed from those of Stanford, additions and changes were made in the course of developing JPL's manipulator system.

The Stanford design consists of a six-jointed, boom-configured manipulator. All six links move simultaneously, providing coordinated motions. The original control technique (Ref. 1) used a full representation of the manipulator's mechanical and inertial characteristics. As development proceeded, it became apparent that the performance was not satisfactory, which dictated changes verified by analysis. Because of the increased control loop response, simpler control techniques could be employed which placed more reliance on standard servo loops to control the motion of the individual links. Eventually, the very complicated model of inertias, reaction torques, and driving torques was eliminated, which resulted in a considerable savings in computer storage and computation time.

SECTION II

EVOLUTION OF THE PRESENT CONTROL SYSTEM

The original system control software, as developed at Stanford, modeled the entire manipulator in terms of inertia, reaction torques, gravity torques, friction torques, and motor characteristics. In essence, it was supposed to compute the torque characteristics necessary to perform a maneuver in an open-loop manner, and if done correctly, the manipulator could move very rapidly with no error. However, position and rate feedback were included to compensate for model errors. The first JPL version of the control system was the same as the Stanford system from which it was copied, except for the addition of tachometers in place of numerical differentiation to obtain rate feedback. Over a period of time, other changes were made which resulted in the present simpler system.

The first modification made at JPL was to change from voltage drive to current drive amplifiers. A complete sampled data analysis done with voltage drive showed that the gains would have to be changed for large changes in inertia regardless of the fact that the inertia was continually computed and used as a gain multiplier. Another advantage of current drive was the elimination of the motor back electromotive force (EMF) compensation. The second modification was to eliminate the friction compensation in the control software and increase the gains for better performance. Unexpectedly high frictional torque was encountered in the harmonic drive speed reduction gears. This was a sinusoid with angular motion, thus making the friction compensation useless since it used only a constant. Also the friction in sliding joint 3 was very erratic. Considerably higher gains were required to increase the response to these large and varying frictional torques.

The sampled data analysis done at that time was for a system with 1-cycle delay since all the signals were computed in sequence, then all were sent out in sequence at the end of the sampled interval, resulting in a full sampling interval delay. The root locus plots clearly indicated that the gains could not be increased very much, so an analysis with no delay was performed. This showed that a much better response could be obtained with no delay. The solution was to change the program to compute each error signal and immediately send out the result to that joint. This procedure was repeated for each joint in turn. The result was a system with approximately 0.10-cycle delay with a sampling rate of 62.5/s. Another analysis was now required which used a variable delay. Its root loci indicated, as expected, a less responsive system than for zero delay, but still considerably better than the original 1-cycle delay system. Later, the sampling rate was doubled to 125/s, which required additional loci with the delay now increased to 0.2. Despite the fact that the analysis indicated sufficient stability margin with new high gain values, lower values were used because the software continually computed very high erratic error signals. This was traced to noise in the system, particularly ground-loop noise. A solution was to introduce the rate error integral gain K_{Iv}. Its effect was to increase the effective position gain ($K_e + K_{Iv}$), but the noise was reduced by the integration process. Again this necessitated an expansion of the analysis and considerably more effort to display the root locus characteristics and transient step responses.

SECTION III

SYSTEM ANALYSIS

The analysis presented here uses conventional techniques for determining system gains and the resultant stability margin, and the steady-state and transient behavior. Modified Z transforms are used since the system employs sampled data with a fixed computation delay which is a small fraction of the total sampling interval. Root locus plots in the Z-plane unit circle indicate relative stability, and responses to step displacements and disturbance torques indicate transient and steady-state response.

A. SYSTEM PARAMETERS AND TRANSFER FUNCTION

A flow diagram of the present manipulator control system is shown in Fig. 1. It indicates the following three distinct portions of each control loop:

(1) The software or digital control located in the General Automation SPC-16/85 minicomputer.

(2) The manipulator joint drive motor, along with its current drive amplifier, and the tachometer and angular position potentiometer for feedback of rotation rate and angle, respectively.

(3) The interface between the computer and the manipulator, consisting of digital-to-analog and analog-to-digital (A/D) converters.

The digital control implies a finite sampling time or computation cycle time shown by the sampler with period T in seconds. The sampling rate is then the reciprocal of T.

Figure 2 replaces the various software and hardware blocks in Fig. 1 with their respective Laplace transforms. A minor point is that the A/D converters do not continuously update but read only every T seconds, which would require that the sampler switches be placed on the other side of the converters. However, the effect is the same, and the sample and hold are done appropriately in the analysis. Figure 2 can be reduced to the simple flow diagram presented in Fig. 3(a).

Figure 3(a) represents the actual control system configuration. The approach here is to analyze this system for stability by deriving the characteristic equation and plotting parametric root loci in the unit Z-plane circle. Along with this, the transfer function for a step displacement and a step disturbance torque will be derived using configurations 3(b) and 3(c), respectively. The transient response to these step inputs can be computed easily from the Z transfer function and plotted using a general-purpose computer with its plotting equipment. The overall sampled data transfer function for Fig. 3(a) is

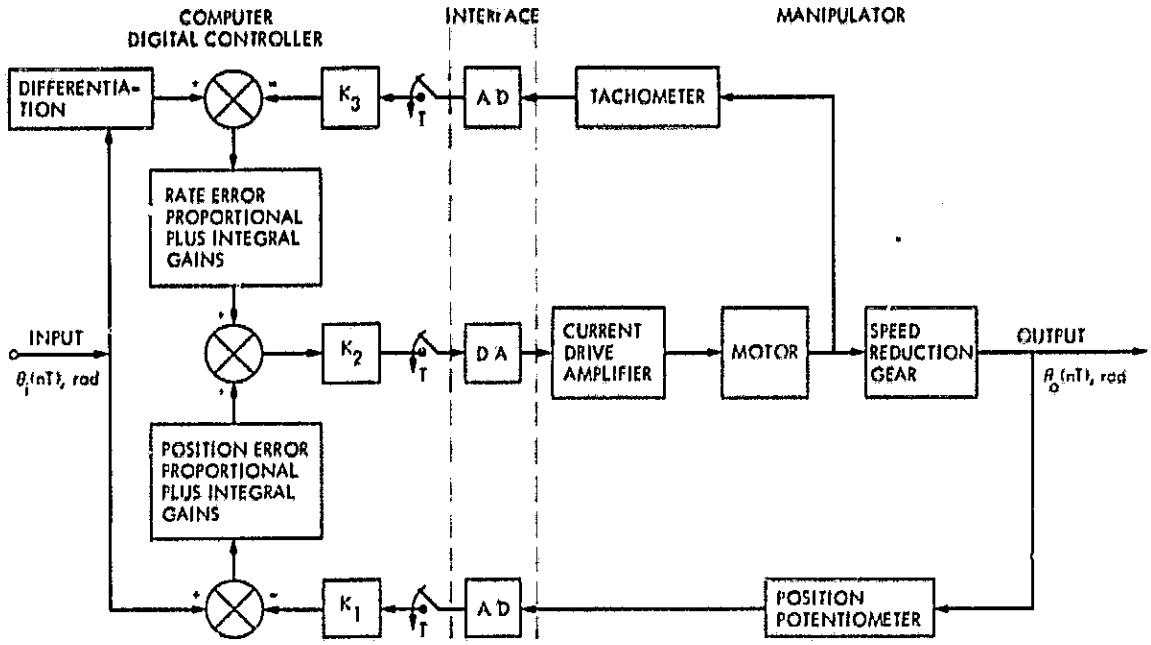

Figure 1. Physical Configuration of Manipulator Control Loops

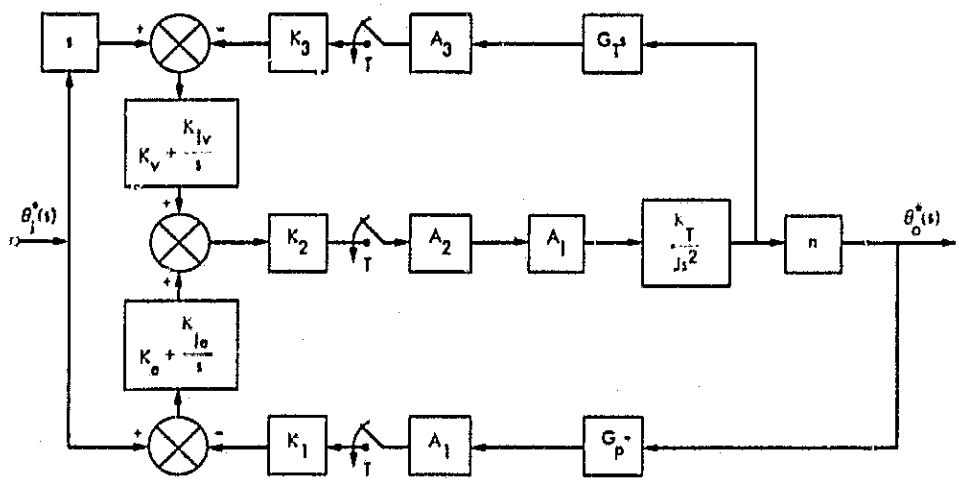

Figure 2. Analysis Configuration of Manipulator Control Loops

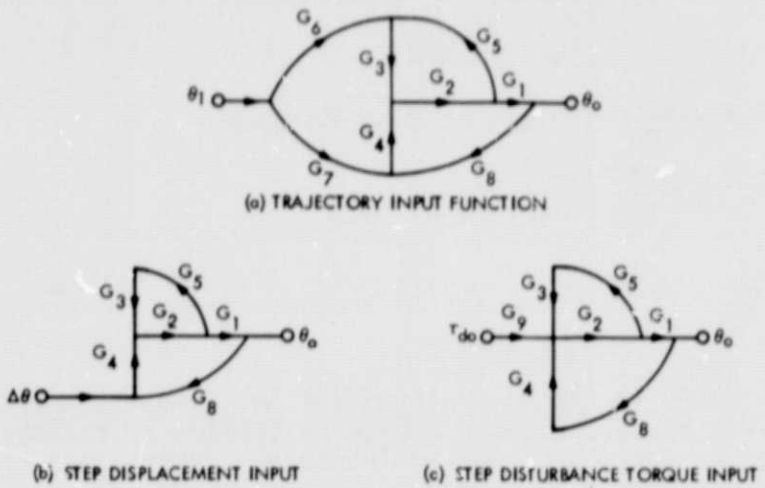

Figure 3. Control System Flow Diagram for Various Inputs

$$\frac{\theta_o^*}{\theta_i^*} = \frac{G_1G_2G_{ho}^*G_4^* + G_1G_2G_{ho}^*G_3^*G_6^*}{1 - G_3^*G_5G_2G_{ho}^* - G_1G_2G_8G_{ho}^*G_4^*} \qquad (1)$$

where the starred transform $G^*(s)$ represents the ordinary Laplace transform of the sampled signal $e^*(t)$.

Referring to Fig. 2, the individual Laplace transfer functions are

$G_1 = n$ Speed reduction gear ratio

$G_2 = K_2A_2A_I \frac{K_T}{Js^2}$ Motor and forward loop gains

$G_3 = K_v + \frac{K_{Iv}}{s}$ Rate error proportional plus integral gains

$G_4 = K_e + \frac{K_{Ie}}{s}$ Position error proportional plus integral gains

$G_5 = -K_3A_3G_Ts$ Rate feedback gain

$G_6 = s$ Analytic differentiation of input function

$G_7 = 1$ Unity gain

$G_8 = -K_1 A_1 G_p$ Position feedback gain

$G_{ho} = \frac{1 - e^{-sT}}{s}$ Zero-order hold

$G_9 = \frac{1}{K_T}$ Constant to convert torque to current, A

As indicated in the definitions for the constant multipliers K_1, K_2, and K_3, these constants are for unitizing or essentially canceling the gains due to the various hardware elements and also to introduce the gain multiplier J'/K_T'. The effect of this is to make each control loop a function of only the gains K_e, K_v, K_{Ie}, and K_{Iv}. Now the following element transfer functions reduce to

$$G_2 = \frac{J'}{K_T'} \frac{K_T}{Js^2} \frac{1}{n}$$

$G_5 = -ns$

$G_8 = -1$

The gear reduction ratio (n) now cancels from the transfer function, but most importantly, each manipulator joint servo loop is dependent only on the multipliers,

K_e Angular position error gain, s^{-2}

K_{Ie} Angular position error integral gain, s^{-3}

K_v Angular rate error gain, s^{-1}

K_{Iv} Angular rate error integral gain, s^{-2}

Thus, if the multiplier J'/K_T' is equal to the reciprocal of the ratio K_T/J (actual motor torque constant/actual total inertia at the motor shaft) for each control loop and the same gain values are used, all manipulator joints will have the same stability margin and identical transient responses. This is a very desirable situation, unless hardware limitations such as an underpowered motor drive dictate decreased gains and slower response for a particular joint.

In general, the K_T parameter for each motor is known quite accurately, but the inertia for some joints can change significantly, as indicated in Table 1. Since the inertia value is no longer computed continuously, a constant average value will be used. The approach is to multiply all four gains by this deviation factor. The effect on stability is easily obtained

Table 1. Values for Unitizing Multipliers K_1, K_2, and K_3, and for Parameters Used in Their Derivation

Parameter	Manipulator Joint					
	1	2	3	4	5	6
A_I, A/V	1.5	1.5	0.5	0.2	0.2	0.05
G_P, V/manip-rad	3.274	3.274	0.21	3.274	3.274	3.274
G_T, V/motor-rad s^{-1}	0.034	0.044	0.354	0.064	0.063	0.025
A_1, input-unit/V	409.6	409.6	409.6	409.6	409.6	409.6
A_2, V/output-unit	0.0195	0.0195	0.0195	0.0195	0.0195	0.0195
A_3, input-unit/V	409.6	409.6	409.6	409.6	409.6	409.6
n (θ_o/θ_m)	0.010	0.010	1	0.0139	0.0139	0.00684
$K_T' = K_T$, motor-oz-in./A	6.8	15.7	40.	10.	10.	4.5
$K_{TO}' = K_T/n$, manip-oz-in./A	680.	1570.	40.	719.	719.	658.
J', oz-in.-s^2 (to motor)	0.0512	0.0640	0.21	0.00312	0.00310	$1.34\ 10^{-4}$
$J_0' = J'/n^2$, oz-in.-s^2	512.	640.	0.21	16.13	16.06	2.86
J_0,[a] oz-in.-s^2 (to manip)	201↔833	508↔1003	0.21	15.1↔17.3	15.9	2.89
J'/K_T', A s^2	$7.53\ 10^{-3}$	$4.07\ 10^{-3}$	$16.5\ 10^{-3}$	$3.12\ 10^{-4}$	$3.10\ 10^{-4}$	$3.0\ 10^{-5}$

Table 1. Values for Unitizing Multipliers K_1, K_2, and K_3, and for Parameters Used in Their Derivation (Continuation 1)

Parameter	Manipulator Joint					
	1	2	3	4	5	6
J_0'/J_0	0.61↔2.6	0.64↔1.3	1.0	0.93↔1.07	1.01	0.99
K_1, manip-rad/input-unit	$7.46\ 10^{-4}$	$7.46\ 10^{-4}$	0.0116	$7.46\ 10^{-4}$	$7.46\ 10^{-4}$	$7.46\ 10^{-4}$
K_2, output-unit s^2	25.7	13.9	0.537	5.75	5.72	4.50
K_3, manip-rad s^{-1}/input-unit	$7.18\ 10^{-4}$	$5.55\ 10^{-4}$	$69.0\ 10^{-4}$	$5.30\ 10^{-4}$	$6.68\ 10^{-4}$	$6.68\ 10^{-4}$
n/J', 1/oz-in.-s^2	0.19	0.16	4.7	4.5	4.5	17.9

[a]Inertia of manipulator with no load in the hand.

Table 1. Values for Unitizing Multipliers K_1, K_2, and K_3, and for Parameters Used in Their Derivation (Continuation 2)

Definition of Parameters		
A_I	≡	current drive amplifier gain
G_P	≡	angular position potentiometer for position feedback
G_T	≡	angular rate tachometer for rate feedback
A_1	≡	A/D converter for position feedback
A_2	≡	D/A converter for error signal to motor
A_3	≡	A/D converter for rate feedback
n	≡	gear, motor to manipulator, stepdown ratio
K_T	≡	nominal motor torque constant
K_T'	≡	value of motor torque constant (referred to motor shaft) used in computing program constant K_2
J'	≡	value of inertia (referred to motor shaft) used in computing program constant K_2
J_0'	≡	value of J' referred to manipulator joint rather than motor shaft
K_{TO}'	≡	value of K_T' referred to manipulator joint
J_0	≡	range of actual inertia referred to manipulator joint
J_0'/J_0	≡	ratio of constant inertia value used in program (for K_2) to actual value as manipulator configuration changes
J'/K_T'	≡	motor characteristic constant used in computing K_2
$K_1 = \frac{1}{A_1 G_P}$	≡	computed constant used to convert units from A/D converter back to radians, and essentially unitize angular position feedback gain

Table 1. Values for Unitizing Multipliers K_1, K_2, and K_3, and for Parameters Used in Their Derivation (Continuation 3)

Definition of Parameters	
$K_2 = \frac{J'}{nA_2A_IK_T'}$	
$= \frac{J_0}{A_2A_IK_{TO}'}$	$\equiv$ computed constant used to convert error signal to proper D/A converter units, and essntially unitize all gains in loop except K_e, K_v, K_{I_v}, and K_{I_e}
$K_3 = \frac{n}{A_3G_T}$	$\equiv$ computed constant used to convert units from A/D converter back to rad/s, and essentially unitize angular rate feedback gain; also to convert feedback from motor rad/s to manipulator rad/s to agree with input signal units

by plotting the resultant root locus. If the stability or transient response is degraded too much, the gains for that particular joint can be reduced or a simple algorithm can be used to compute the inertia change as a function of manipulator joint configuration. An additional factor to consider here is the change in inertia when manipulating a large object.

1. Comments on Joint 3

Joint or link 3 is the only sliding rather than rotational joint. It has the conventional motor drive, with a 0.563-in. radius shaft for driving the linear motion arm. Thus, the weight of the moving part is essentially the mass, and the radius of gyration is the radius of the drive shaft or gear. The joint can then be treated like all the rest in terms of servo control and computation of K_1, K_2, and K_3. Both its rate and position feedback are obtained from rotary sensors mounted on the motor shaft, so that there is no gear reduction for position as with all the other joints. The input function in terms of inches has to be converted to radians by dividing by the radius (0.563 in.).

2. Truncation of A/D and D/A Converters

All the A/D converters are 13-bit devices, 1 sign bit and 12 data bits. A 10-V input into the A/D results in full-scale output or 2^{12} = 4096 output units. Since the angular position potentiometer sensi-

tivity is 3.274 V per manipulator radian, full-scale output represents ± 3.054 rad. The resultant truncation is $\pm 3.054/4096 = 0.745$ mrad for all joints except 3. The angular rate sensitivity (referred to the manipulator rather than the motor) and the resultant truncation differs for some joints as indicated in Table 2.

The D/A converter is a 10-bit device with one sign bit and 9 data bits. Full-scale input of $\pm 2^9 = \pm 512$ results in 10 V output. The truncation is then 0.0195 V, which can be converted to amps using the A_I values from Table 1 or to other units using the proper parameters.

B. STABILITY

The characteristic equation is obtained from Eq. (1) by combining the given Laplace transforms of G_1 through G_8 to obtain all the starred transforms, and then converting them to their corresponding Z transforms. At this point, it should be made clear that modified Z transforms will be used since we are analyzing a sampled data system with fixed delay; i.e., the position and rate feedback data for one manipulator joint are read in essentially simultaneously, and operated on to compute the output error signal, which is then sent out to the drive motor prior to repeating the process for the remaining five joints. Thus, a fixed computation delay T_D is present, and the total sampling interval T is determined by the time required to process all six joints.

Table 2. Truncation of A/D Converters

	Full-scale rate		Rate truncation	
Joint	motor rad/s	manip rad/s	mrad/s	deg/s
1	294	2.94	0.72	0.041
2	227	2.27	0.55	0.032
3	2.82	2.82	0.69	0.039
4	156	2.17	0.53	0.030
5	159	2.21	0.54	0.031
6	400	2.74	0.67	0.038

The individual modified Z transforms for the denominator of Eq. (1) are:

$$-G_5G_2G_{ho}(Z) = T\,\frac{mZ - m + 1}{Z(Z-1)}\,\frac{K_TJ'}{JK_T'}$$

$$-G_1G_2G_8G_{ho}(Z) = \frac{T^2}{2}\,\frac{m^2Z^2 + Z(-2m^2 + 2m + 1) + m^2 - 2m + 1}{Z(Z-1)^2}\,\frac{K_TJ'}{JK_T'}$$

$$G_3(Z) = -\,\frac{(K_v + K_{Iv}T)Z - K_v}{(Z-1)}$$

$$G_4(Z) = -\,\frac{(K_e + K_{Ie}T)Z - K_e}{(Z-1)}$$

The characteristic equation has the form

$$A_4Z^4 + A_3Z^3 + A_2Z^2 + A_1Z + A_0 = 0 \qquad (2)$$

where

$$A_4 = 1$$

$$A_3 = -3 + m(C_2 + C_3) + m^2(C_1 + C_4)$$

$$A_2 = 3 + (1 + 2m - 3m^2)C_1 + (1 - 3m)C_2 + (1 - 2m)C_3 + (1 + 2m - 2m^2)C_4$$

$$A_1 = -1 + m(3m - 4)C_1 + (3m - 2)C_2 + (m - 1)C_3 + (m - 1)^2C_4$$

$$A_0 = -(m - 1)^2C_1 + (1 - m)C_2$$

and

$$C_1 = \frac{1}{2}K_eT^2\,\frac{K_TJ'}{JK_T'}$$

$$C_2 = K_vT\,\frac{K_TJ'}{JK_T'}$$

$$C_3 = K_{Iv}T^2\,\frac{K_TJ'}{JK_T'}$$

$$C_4 = \frac{1}{2}K_{Ie}T^3\,\frac{K_TJ'}{JK_T'}$$

$$m = 1 - \frac{T_D}{T}$$

$$\frac{T_D}{T} = 0.1 \quad \left(\text{for } T = \frac{1}{62.5}\ \text{s}\right)$$

$$\frac{T_D}{T} = 0.2 \quad \left(\text{for } T = \frac{1}{125}\ \text{s}\right)$$

The next step is to program Eq. (2) and compute the roots as a function of the gains K_e, K_v, K_{Iv}, K_{Ie}, the sampling interval T, and the delay from zero to one full cycle (T). An interesting presentation is given here for the case of zero delay.

The Z-plane loci for constant K_v or constant K_e are conveniently circles with origins at -1 and +1, respectively. The two radius equations are

$$r_v^2 = 4 - 2K_vT - K_{Iv}T^2$$

$$r_e^2 = (K_e + K_{Iv})T^2$$

where the gains are as defined previously. These expressions are exact for no integral gain ($K_{Ie} = 0$), but they still apply for a large range ($0 \longrightarrow 60{,}000$) of K_{Ie} since the locus of the complex roots changes little, and only the real root moves along the real axis as K_I increases. This has, of course, been checked using Eq. (2) with no delay (m = 1).

C. TRANSIENT AND STEADY-STATE STEP RESPONSE

Section B introduced the system characteristic equation, which, for specific gain values, indicates the relative stability in terms of location of the roots of this equation in the Z-plane unit circle. This information is sometimes sufficient in itself, but usually it is desirable to analyze the control system response to step inputs. In this case, we are interested in response to steps of position $\Delta\theta$ and disturbance torque τ_{do}. The transient response in terms of rise time, overshoot, and damped oscillation frequency, along with the final steady-state response to these inputs, is very useful information. Also, the actual measured response obtained by applying these step inputs to the physical system is a good indication of the accuracy of the system model and the understanding of its performance.

1. Step Displacement Transfer Function

Equation (1) can be used to obtain the desired transfer function. However, a slight modification is necessary since the second term in the

numerator contains the differentiation element (G_6). Normal inputs are polynomials in joint angle as a function of time (nT). Thus, the analytic differential can be easily computed, but a step input is never used by the trajectory program and certainly not differentiated. Therefore, we can think of an input step $\Delta\theta_i$ as a displacement error which occurs when the loop is initially closed. The result is the elimination of the second term in the numerator since it has no effect on this input.

For a step displacement input

$$\Delta\theta_i(Z) = \Delta\theta \frac{Z}{Z - 1}$$

the output response is

$$\theta_o(Z) = \frac{\Delta\theta_i Z[m^2Z^2 + (-2m^2 + 2m + 1)Z + (m - 1)^2][(C_1 + C_4)Z - C_1]}{(Z - 1)\,[A_4Z^4 + A_3Z^3 + A_2Z^2 + A_1Z + A_0]} \quad (3)$$

where all the parameters are as defined in Section B. To obtain the transient response as a function of nT, it is necessary to expand Eq. (3) to the following form:

$$\theta_o(Z) = \frac{\Delta\theta_i(B_4Z^4 + B_3Z^3 + B_2Z^2 + B_1Z)}{Z^5 + (A_3 - A_4)Z^4 + (A_2 - A_3)Z^3 + (A_1 - A_2)Z^2 + A_0 - A_1)Z - A_0} \quad (4)$$

where

$$B_4 = m^2(C_1 + C_4)$$

$$B_3 = (1 + 2m - 3m^2)C_1 + (1 + 2m - 2m^2)C_4$$

$$B_2 = m(3m - 4)C_1 + (1 - m)^2C_4$$

$$B_1 = -(1 - m)^2C_1$$

Division of Eq. (4) is easily programmed on a computer and the step response obtained for a specific set of input parameters. If the final value theorem is applied to Eq. (3),

$$\lim_{n\to\infty} \theta_o(nT) = \lim_{Z\to 1} \frac{(Z - 1)}{Z}\theta_o(Z)$$

$$= \Delta\theta_i \frac{2C_4}{2C_4} = \Delta\theta_i$$

as would be expected for an input step $\Delta\theta_i$. But if K_{Ie} is zeroed,

$$\underset{n\to\infty}{\theta_o(nT)} = \frac{2C_1}{2C_1 + C_2}\Delta\theta_i = \frac{K_e}{K_e + K_{Iv}}\Delta\theta_i$$

indicating that the rate integral gain (K_{Iv}) has to be zero or the output will not reach $\Delta\theta_i$.

2. Step Torque Disturbance Transfer Function

Each manipulator joint control system is subject to disturbance torques, some joints more than others. These torques can be due to the hand encountering an object, gravity effects, inertia reactions from other joints during movement, and, in this case, very large and changing friction torques in the harmonic drive reduction gears. It is important to know the transient and steady-state response to these torques, which are generally not pure step inputs, but the step response analysis is quite sufficient for selecting proper gains for optimum response in conjunction with stability margin requirements.

The output response for an input torque is

$$\theta_o^* = \frac{G_2G_1G_9\tau_{do}^*}{1 - G_3^*G_5G_2G_{ho}^* - G_1G_3G_8G_{ho}G_4^*} \tag{5}$$

The torque τ_{do} refers to an output torque and has to be multiplied by the gear stepdown ratio n to reference it to the motor shaft. Then it must be multiplied by the torque-to-current conversion factor G_9, which results in a numerator

$$G_2G_1G_9\tau_{do}^*(s) = \frac{n^2}{K_T}G_2\tau_{do}(s)$$

Here, G_2 is the motor transfer function K_T/Js^2 and is not multiplied by the constant J/K_T as in the previous derivation for an input θ_i (Eq. 1). Letting the torque input be a step torque τ_{do}/s results in a numerator

$$G_2G_1G_9\tau_{do}^*(s) = \frac{n^2\tau_{do}}{Js^3} \tag{6}$$

The Z-transform of Eq. (6) is

$$G_2G_1G_9\tau_{do}(Z) = \frac{n^2\tau_{do}T^2[m^2Z^2 + (-2m^2 + 2m + 1)Z + (m - 1)^2]}{2J(Z - 1)^3} \tag{7}$$

Making all the denominator substitutions in Eq. (5) as was done in Section C-1 results in a factor of Z transposed to the numerator, and the final transfer function for a step torque is

$$\theta_o(Z) = \frac{n^2\tau_{do}T^2}{2J} \frac{[m^2Z^2 + (-2m^2 + 2m + 1)Z^2 + (m - 1)^2Z]}{A_4Z^4 + A_3Z^3 + A_2Z^2 + A_1Z + A_0} \qquad (8)$$

where the denominator coefficients are as defined in Section B and τ_{do} has units of ounce-inches if J is in ounce-inch-seconds squared. Again the transient response can easily be obtained by programming the division of Eq. (8) for a specific set of parameters.

It is of interest to apply the final value theorem to Eq. (8), assuming nonzero values for all the gains:

$$\lim_{n\to\infty} \theta_o(nT) = \lim_{Z\to 1} \frac{(Z - 1)}{Z} \theta_o(Z) = 0$$

Thus, for a step torque, a transient error in θ_o occurs but decays to zero. But if the position error integral term K_{Ie} is zero, the output error becomes

$$\lim_{n\to\infty} \theta_o(nT) = \frac{n^2\tau_{do}T^2}{J(2C_1 + C_3)} = \frac{n^2\tau_{do}K_T'}{J'K_T(K_e + K_{Iv})} \qquad (9)$$

For a 10,000-oz-in. step torque, an inertia (J) of 0.034 oz-in.-s^2 (J' multiplier = 0.034 and $K_T'/K_T = 1$), a gear reduction ratio of 1/100, and a K_e value of 3600, the steady-state position error from Eq. (9) is 0.47 deg. With any value of K_{Ie} inserted, this error decays to zero, but a larger value of K_{Ie} will cause it to decay faster. Some of these torque response characteristics are given in the Appendix. It should be noted from Eq. (9) that the magnitude of the steady-state error with no K_{Ie}, and even the magnitude of the transient response to a step torque with K_{Ie} in, will vary for each joint as a function of the gain multiplier J' and the ratio K_T'/K_T. Generally, K_T'/K_T will be unity; therefore, the error is determined by the factor n^2/J' since each joint will have the same value of K_e and K_{Iv} as selected from the root locus plots.

The above discussion of the transient position error due to a disturbance torque indicates why it is important to analyze such responses as well as select proper gains for stability. Every manipulator joint should operate with the same gains (K_e, K_v, K_{Ie}, K_{Iv}) and have the same locus of roots, but as indicated above, the error due to a disturbance torque will be a function of the factor n^2/J', which differs for most of the joints, as indicated in Table 1. It is important to consider this, since reaction torques are reflected back to each joint during movement. Of course, these are reduced by the gear reduction ratio n. A more significant effect is from the varying friction torque. This torque is not reduced by n and is a real problem if it is high and the gains are low, resulting in an undesirable rough motion. Table 1 indicates why joints 3 through 6 are particularly susceptible to this type of disturbance as shown by their relative high values of n/J'. The parameter n is not squared here since it is assumed that the friction torque is not reduced by n, but the resulting transient position error is referred to the output by the remaining n factor.

SECTION IV

DISCUSSION OF STABILITY AND TRANSIENT RESPONSE AS A FUNCTION OF GAINS

The data to be summarized here consists of a series of root locus plots and transient step responses presented in the Appendix. These are only a very small fraction of the total plots generated during the extended study of this system. No attempt will be made here to analyze and compare each successive system. The important point is to analyze the present and, it is hoped, final system configuration. This final system is one which has a sampling rate of 125 per second and about 20% delay. Unfortunately, the increase in sampling rate from 62.5 to 125 occurred after the analysis was completed. The bulk of the plots therefore pertain to a system with a sampling rate of 62.5 and 10% delay. A few computer runs were made at the higher sampling rate to justify a reasonable set of gains, but a thorough set of locus plots was not obtained. This is not necessarily a problem since the data presented should give a good insight into the system response.

The discussion of stability and transient response here will refer to each figure from the Appendix in turn.

The Z-plane unit circle is displayed in Fig. A-1 with constant damping ratio and constant damped frequency radii superimposed. For a simple second-order system, the damping ratio (ζ) and damped frequency (ω_d) apply directly to any set of complex roots in the unit circle. Higher-order systems will not produce the simple second-order response, but the complex pole location is still very informative since the relative location of two sets of poles gives some insight into the transient response to displacement errors and disturbance torques. The damped frequency, which is indicated as a function of the sampling frequency, is particularly important in estimating the response time to input disturbances.

Zero-delay loci are shown in Fig. A-2 to indicate the very high gains and fast response possible. Of coure, zero delay is not obtainable at such high sampling rates since it takes time to compute the error signals. The interesting aspect is that the loci are circles with origins at -1 and +1 and are easily drawn for any value of K_e, K_v, and K_{Iv}. It should be noted that these loci apply only for zero position integral gain K_{Ie} and a sampling rate of 62.5 per second.

The zero-delay loci in Fig. A-3 are presented only to show the change for the higher, 125 sampling rate. The radii r_v and r_e for a specific complex pole location are shown to indicate that, given these magnitudes and selecting one gain, the other two gains can be computed using the given equation.

An arbitrary point on the loci of Fig. A-3 was selected in Fig. A-4 and the integral gain then varied from zero to 80,000. The system is still stable (for zero delay), but obviously the complex root moves toward lesser damping and stability margin as the integral gain increases.

Figure A-5 presents the first loci with delay other than zero. The delay T_D/T is varied from zero to 0.30 to show how the system becomes unstable as the delay becomes larger than 0.30. The zero-delay point should coincide with the pole location for this set of gains in Fig. A-3.

In Fig. A-6, we have complete loci for a 10% delay and sampling rate of 60 per second. It indicates how radically the loci for zero delay in Fig. A-3 distort as the delay changes from zero. These loci are only for one pair of complex roots. There is another pair of complex roots at the lower frequency, but it is not shown here.

Both complex roots are shown in Fig. A-7 for three sets of gains. The position integral gain K_{Ie} is then varied from zero to 30,000. The interesting point here is that the higher-frequency complex pole hardly moves, but the lower-frequency one, which is indicative of the system response to a step torque, moves toward lower damping, which implies more overshoot in the step response.

Since the inertia is no longer computed, the average value used may not always equal the actual changing value. This has the effect of multiplying all the gains by the ratio J'/J. Figure A-8 shows the destabilizing effect and the interesting fact that one root becomes less stable as J'/J increases, but the other root becomes less stable as J'/J decreases.

Figure A-9 shows complete loci for 10% delay and the rate integral gain K_{Iv} set to 1000. It should be compared to Fig. A-6 to show how the loci change as K_{Iv} is changed from zero. Other loci were plotted for values of K_{Iv} larger than 1000 and indicate a shift upward toward less stability, as would be expected.

Both complex roots could not be shown in Fig. A-9; therefore, three sets were selected in Fig. A-10 to indicate their movement as the position integral gain K_{Ie} is varied from zero to 30,000. This is a repetition of Fig. A-7 only with different gains; in particular, K_{Iv} is now 1000 instead of zero. The results are similar in that the higher-frequency root changes little, but the lower-frequency root moves toward less damping.

The set of loci in Fig. A-11 is the same as that in Fig. A-8, only for different gains, and K_{Iv} is equal to 1000 rather than zero. Again, the higher-frequency root moves toward less damping as the ratio J'/J increases, but the lower-frequency root moves toward less damping as J'/J decreases.

In Fig. A-12, the first loci for a sampling rate of 125 per second show the same destabilizing effect as the delay changes from zero to 30%. The gain sets were used arbitrarily only for illustration since neither set is very stable as the delay is much above 10%.

The loci shown in Fig. A-13 can be compared to those in Figs. A-4 and A-10, which also show the effect of varying the position integral gain K_{Ie}. The sampling rate here is 125 per second, and

the gain sets were arbitrary, although all three sets could be used. However, set A would have to use a reduced K_{Ie}, probably less than 40,000.

The four step displacement responses in Fig. A-14 show the faster response with larger position gain K_e and also the overshoot increases with added position integral gain K_{Ie}. These and the ones shown in Fig. A-15 are mainly for comparison purposes since the delay here is zero.

The faster response gain set from Fig. A-14 is used in Fig. A-15 to illustrate the better response, to a step torque disturbance, as the position integral gain is increased. However, response D indicates possibly undesirable overshoot as K_{Ie} gets very large. Also, one has to consider the consequent position error overshoot shown in Fig. A-14 as K_{Ie} increases in magnitude.

The responses in Figs. A-16 and A-17 are more realistic than the previous two since the delay is 10% with a sampling rate of 60 per second. This is the actual case with the manipulator, unless the 125-per-second sampling rate is used, which means the delay is 20%. Figure A-16 is interesting in that it shows the effect of the rate integral gain K_{Iv} on the position step response. In general, a large value of K_{Iv} will slow the position step response and eliminate the overshoot. As K_{Ie} is increased, the response increases but still avoids any significant overshoot. Response A shows that with zero integral gain the response will reach only a fraction of the input, by the ratio of $K_e/(K_e + K_{Iv})$.

The response curves in Fig. A-17 clearly show the rapid increase in recovery from a step torque as the position integral gain (K_{Ie}) is increased. The maximum value used is determined by the amount of overshoot one is willing to tolerate.

SECTION V

SUMMARY AND CONCLUSIONS

The sampled data control system used for each of the joints in the JPL manipulator has been described in detail in terms of root locus plots and transient step responses. The mathematical derivations of the various transfer functions are presented, as are all the hardware parameter values. The derivations are for a sampled data system with fixed delay, employing position and rate feedback and current drive for the d.c. drive motor in each joint. Position and rate integrals are computed in the manipulator software, as is the input drive function which defines the joint movements as a function of time.

A small fraction of the root locus plots generated is presented in the appendix, and indicates relative stability as a function of:

(1) Computation delay (10 to 30% of sampling interval).

(2) Position gain, rate gain, position integral gain, and rate integral gain.

(3) Inertia change (±40%).

(4) Sampling rate (62.5 and 125 per second).

A sample of the transient responses to input steps of position and torque is presented in the appendix. These transient responses indicate the response time variation as a function of the position and integral gains.

Based on the data presented here, it can be concluded that the performance of the manipulator can be made to conform to criteria calling for very fast response by increasing the gains properly, as indicated in the root locus plots and transient responses; e.g., a response time constant of less than 0.1 s can be obtained with a sampling rate of 60 per second.

An important feature of this analysis is that the various hardware gains and parameters such as inertia of motor torque constant have all been normalized by using their reciprocal values as gain multipliers in the software. Thus the gain values used throughout this analysis will apply to any similar control system after its hardware gains have similarly been eliminated or considered as part of the total loop gain defined here.

REFERENCE

1. Markiewicz, B. R., "Analysis of the Computed Torque Drive Method and Comparison With Conventional Position Servo for a Computer-Controlled Manipulator," Technical Memorandum 33-601, Jet Propulsion Laboratory, Pasadena, Calif., March 15, 1973.

APPENDIX

ROOT LOCI AND TRANSIENT RESPONSE CHARACTERISTICS

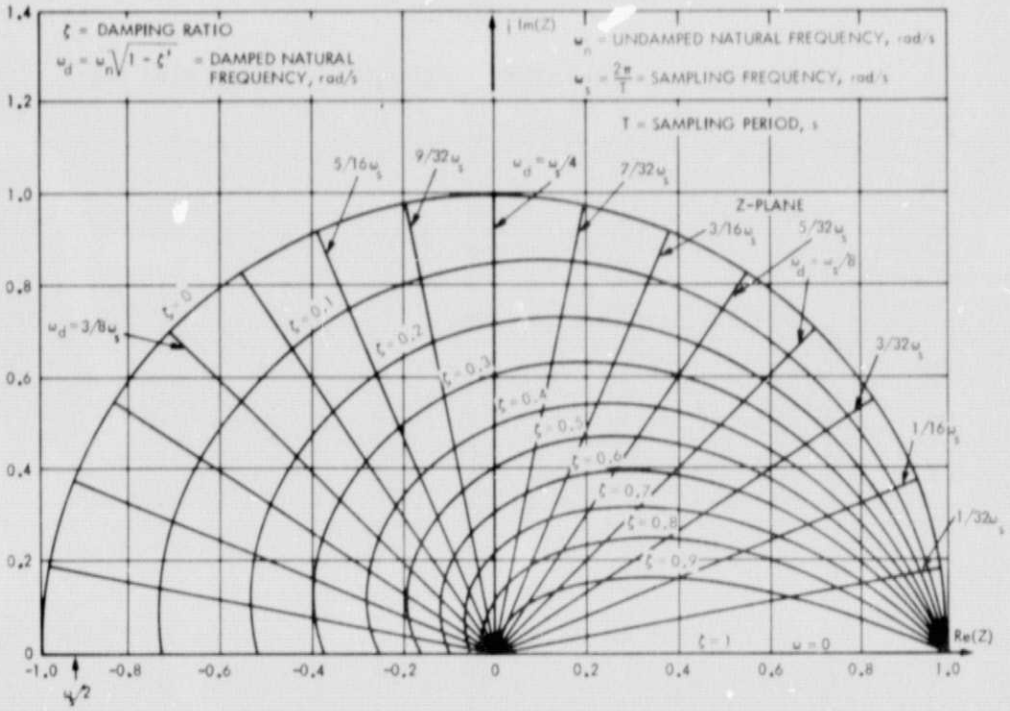

Figure A-1. Z-Plane Unit Circle With Constant Damping Ratio Characteristics and Constant Damped Natural Frequency Characteristics

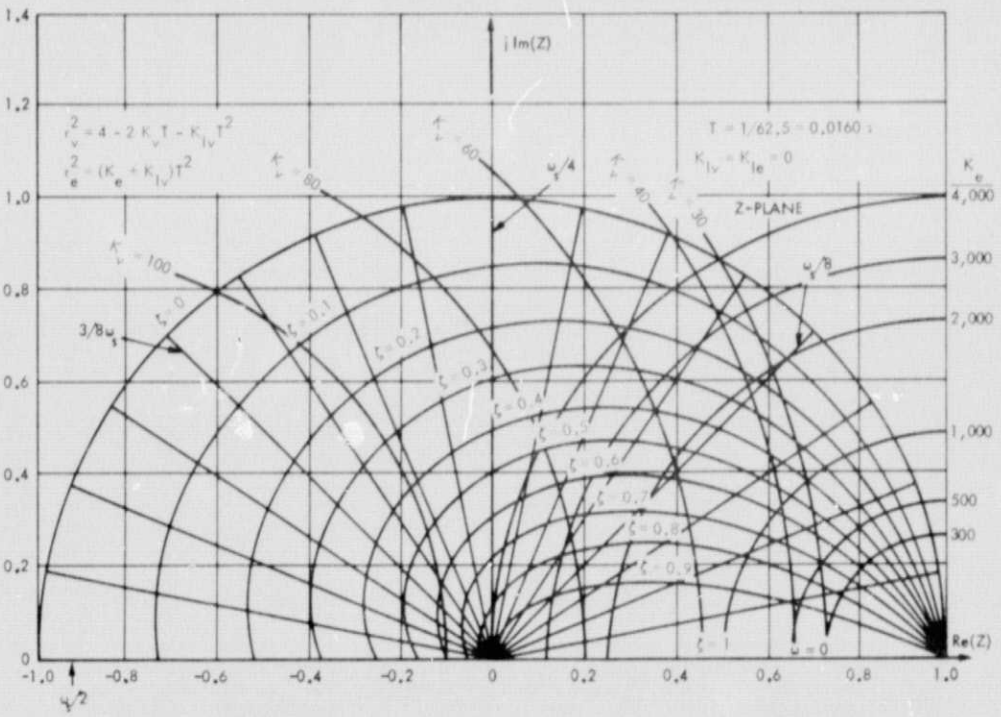

Figure A-2. Loci for Zero Delay and Zero Integral Gains With Sampling Rate of 62.5 per Second

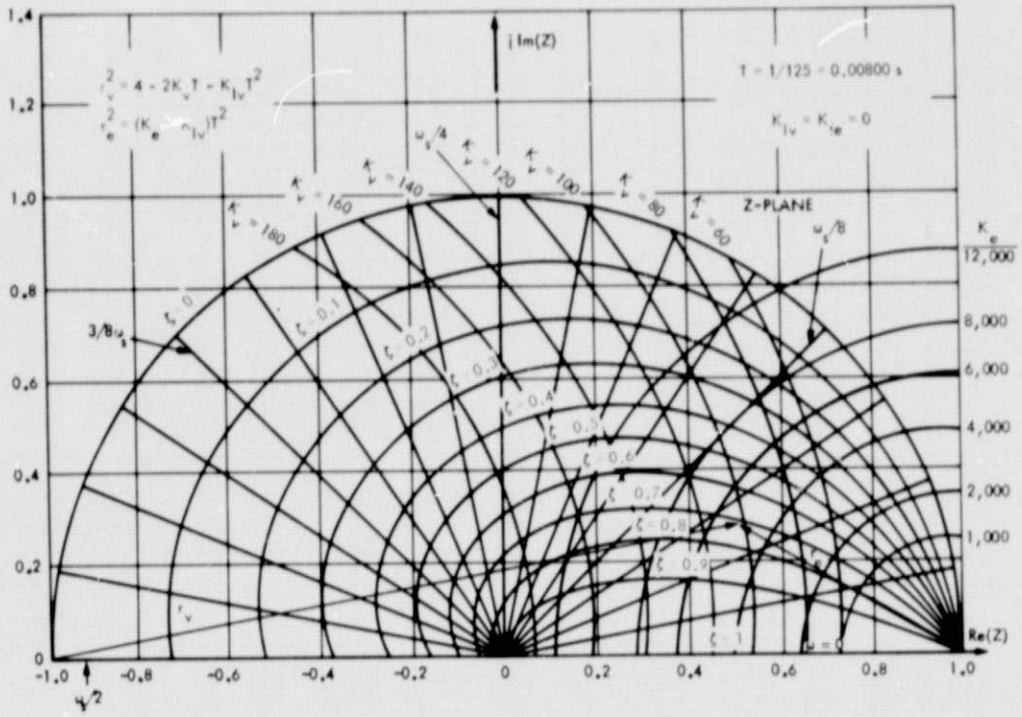

Figure A-3. Loci for Zero Delay and Zero Integral Gains With Sampling Rate of 125 per Second

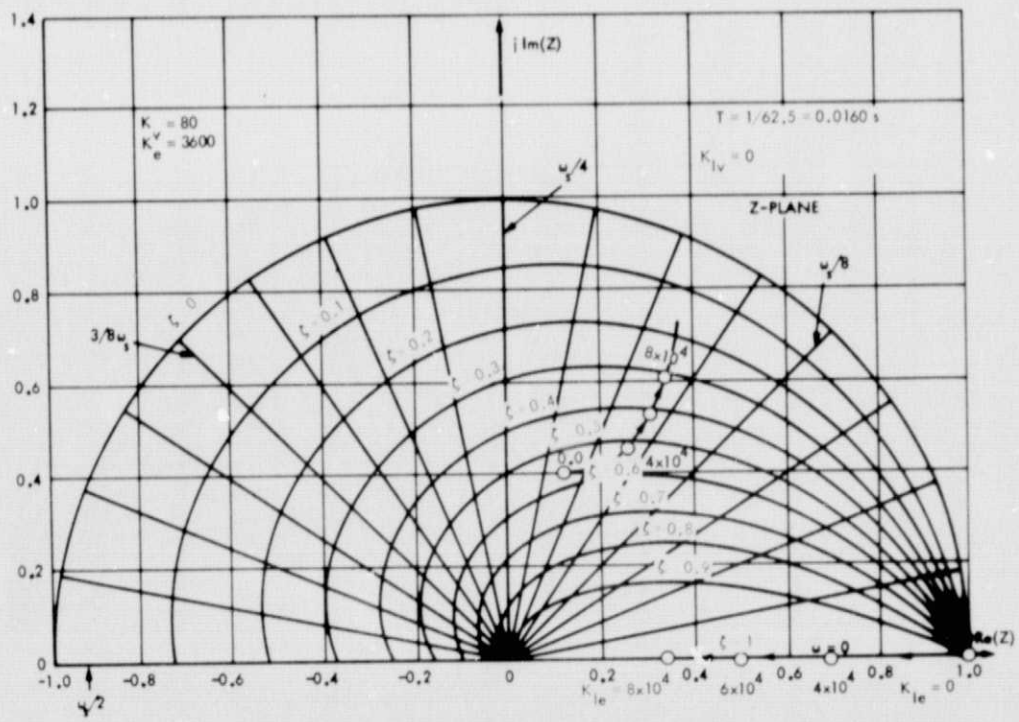

Figure A-4. Locus for Zero Delay as Function of Integral Gain K_{Ie}

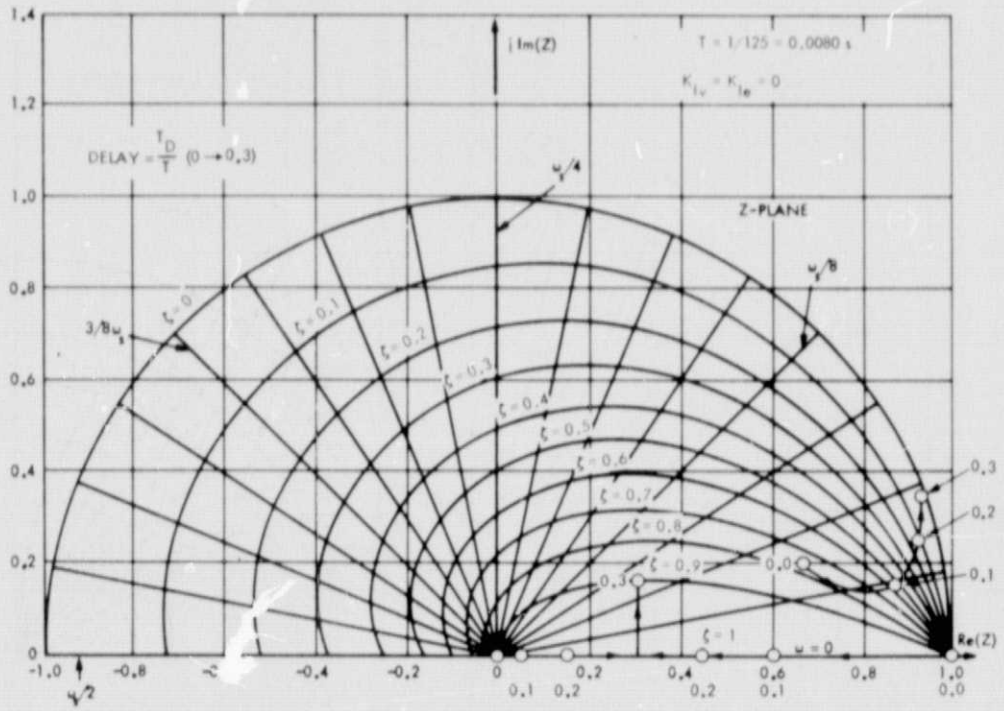

Figure A-5. Locus as Function of Delay with K_e = 24,000, K_v = 75, and T = 0.008 s

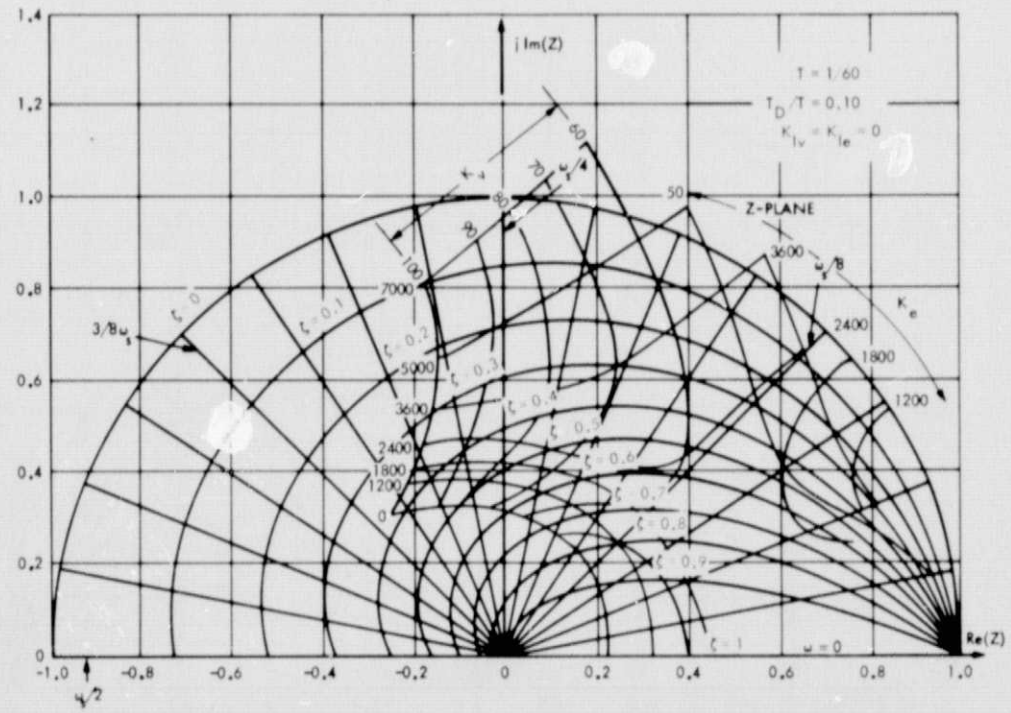

Figure A-6. Loci for 10% Delay and Zero Integral Gains With Sampling Rate of 60 per Second

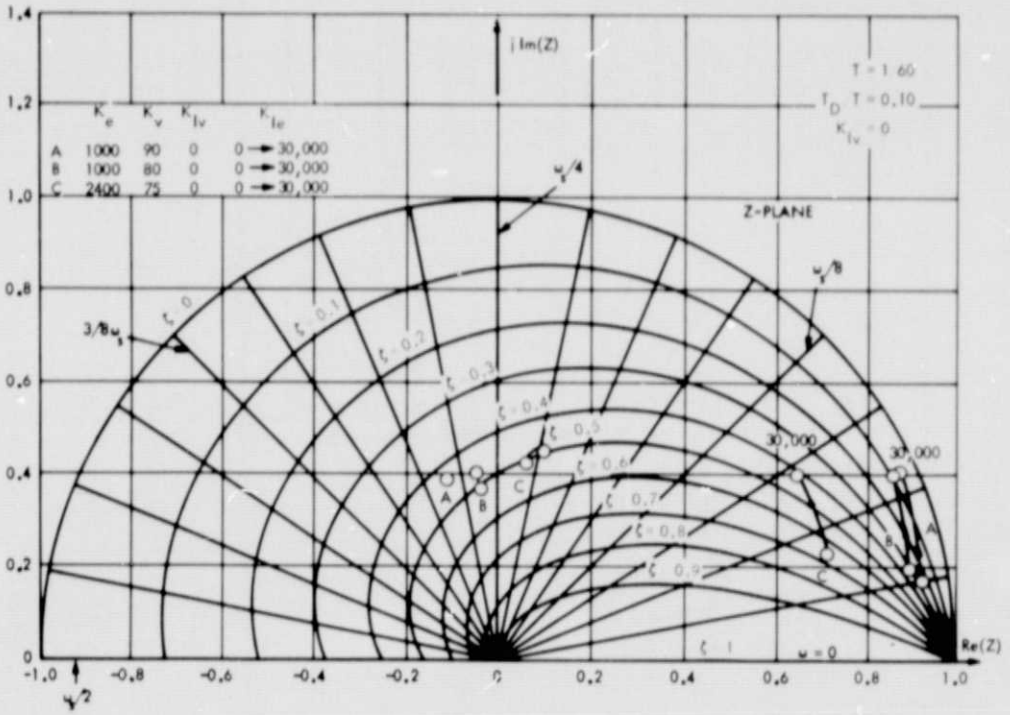

Figure A-7. Typical Loci of Both Complex Roots With 10% Delay as Function of Integral Gain K_{Ie}

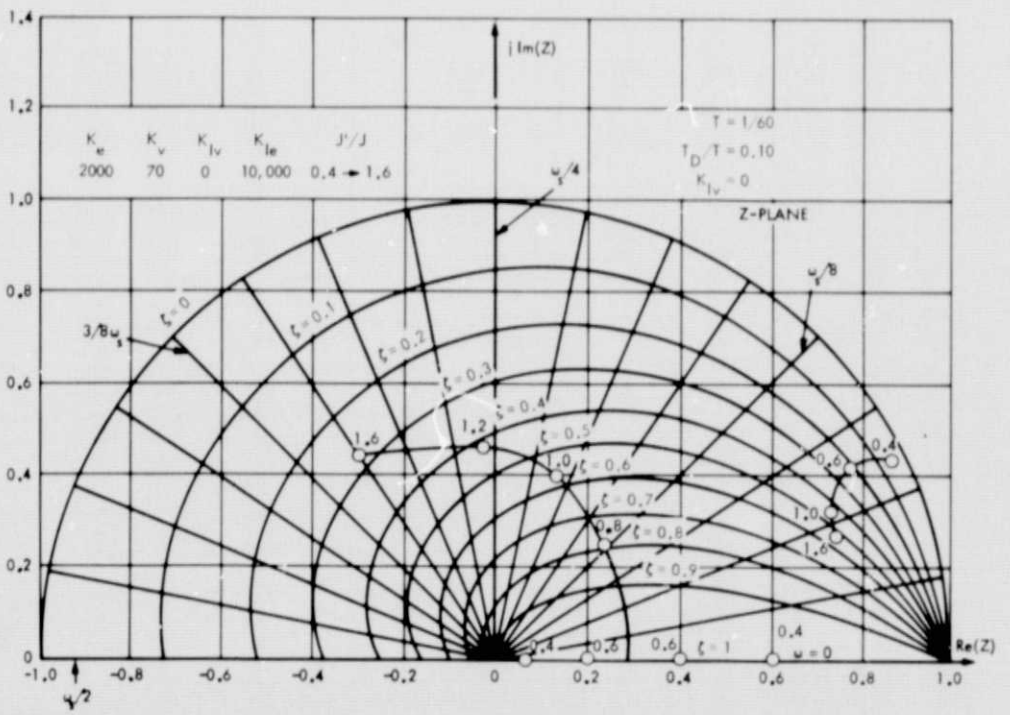

Figure A-8. Typical Loci of Both Complex Roots as Function of Ratio of Inertia Multiplier J′ to Actual Inertia J

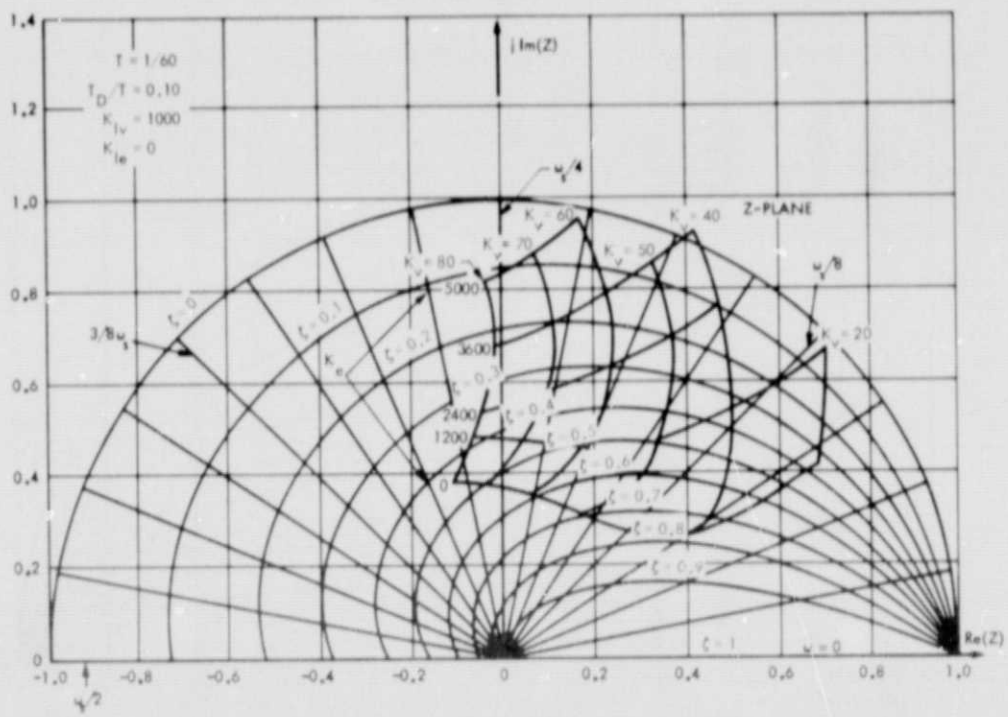

Figure A-9. Loci for 10% Delay, K_{Iv} = 1000 and Zero K_{Ie} With Sampling Rate of 60 per Second

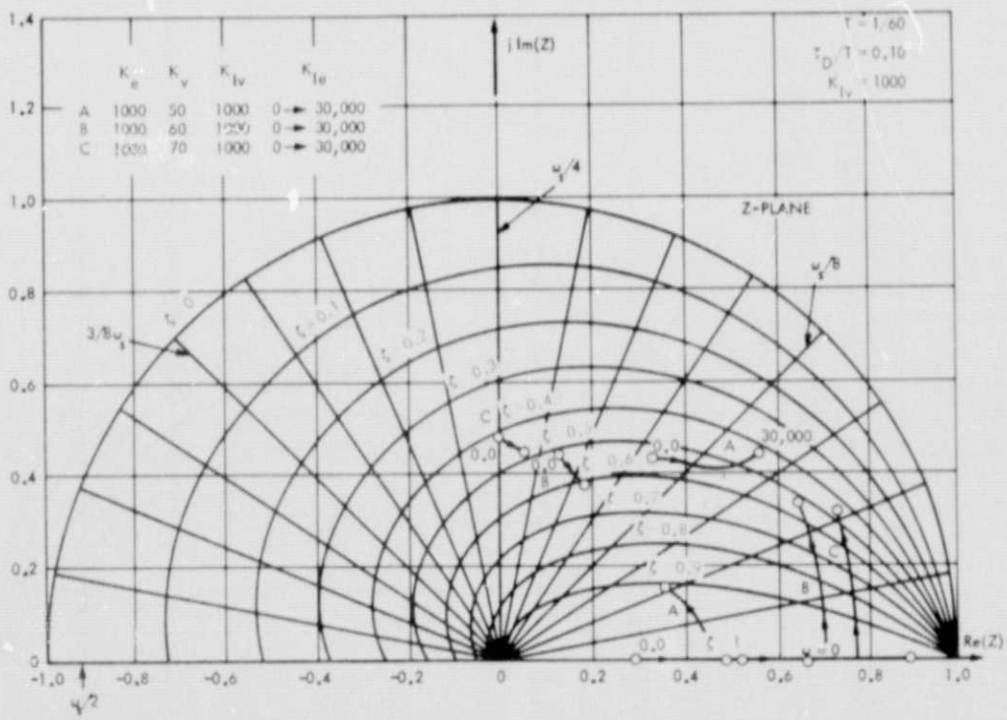

Figure A-10. Typical Loci of Both Complex Roots With 10% Delay and K_{Iv} = 1000 as Function of Integral Gain K_{Ie}

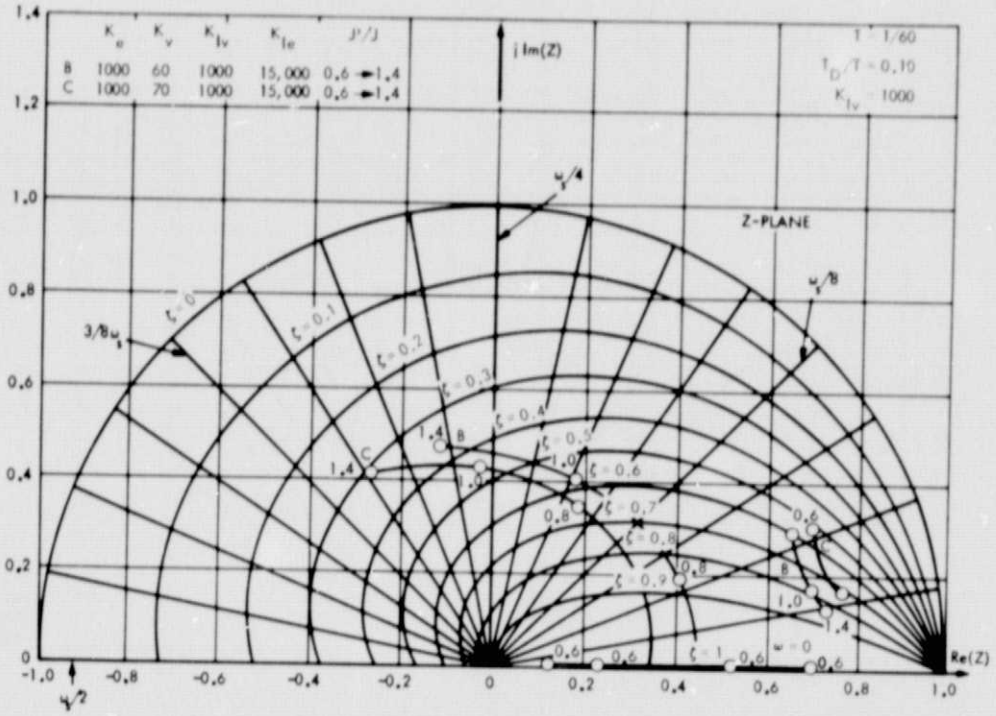

Figure A-11. Typical Loci of Both Complex Roots as Function of Ratio of Inertia Multiplier J' to Actual Inertia J

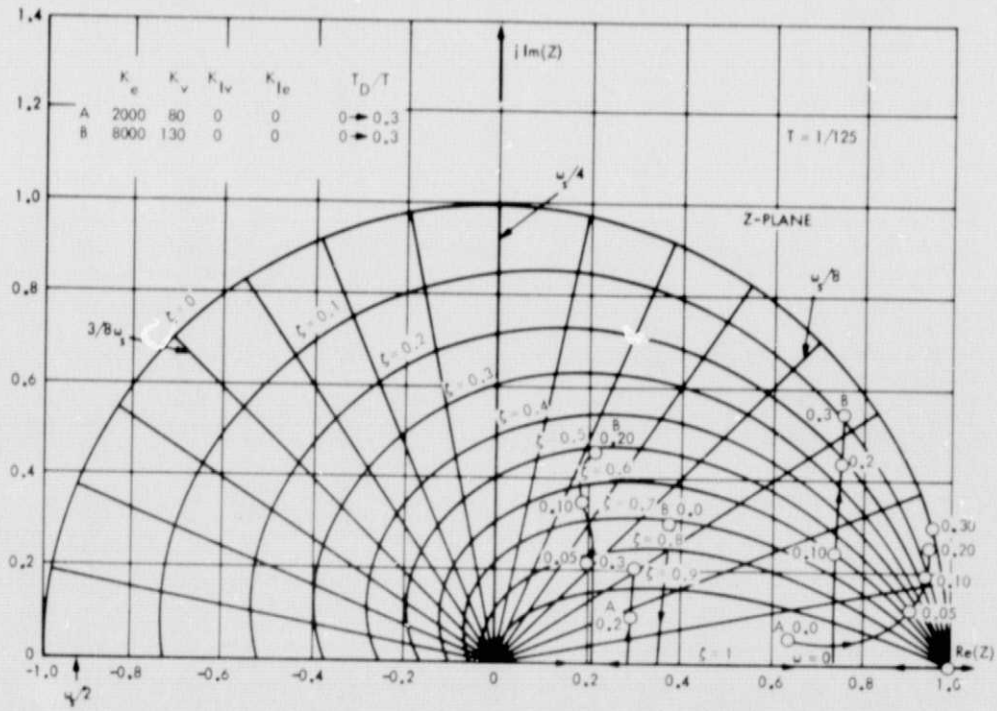

Figure A-12. Typical Loci as Function of Delay With Sampling Rate of 125 per Second

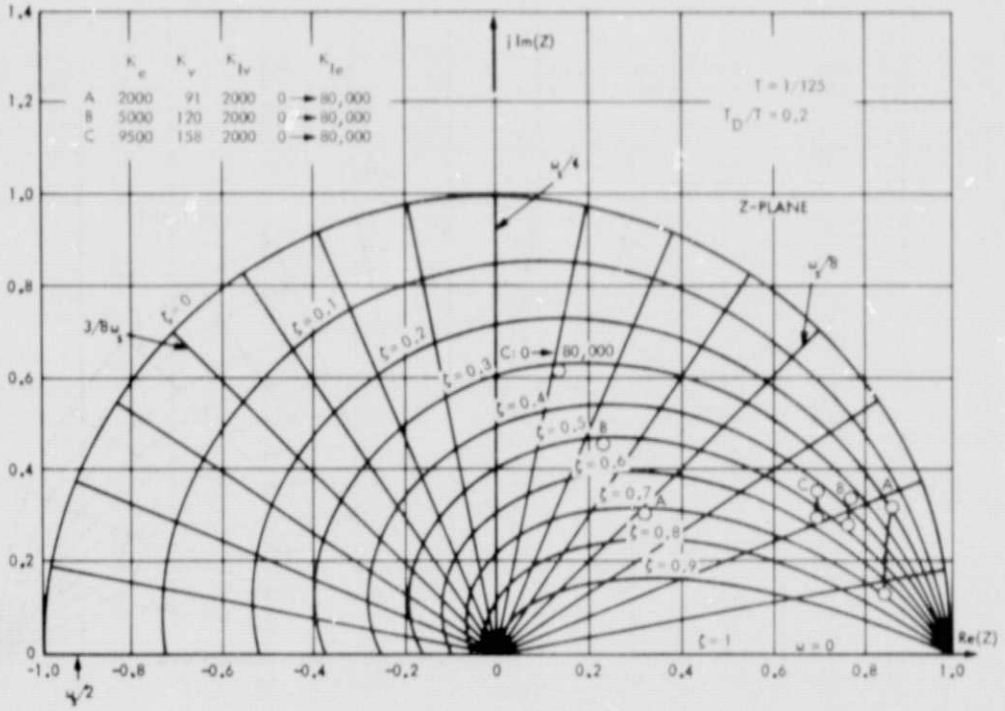

Figure A-13. Typical Loci as Function of Integral Gain K_{Ie} With Sampling Rate of 125 per Second

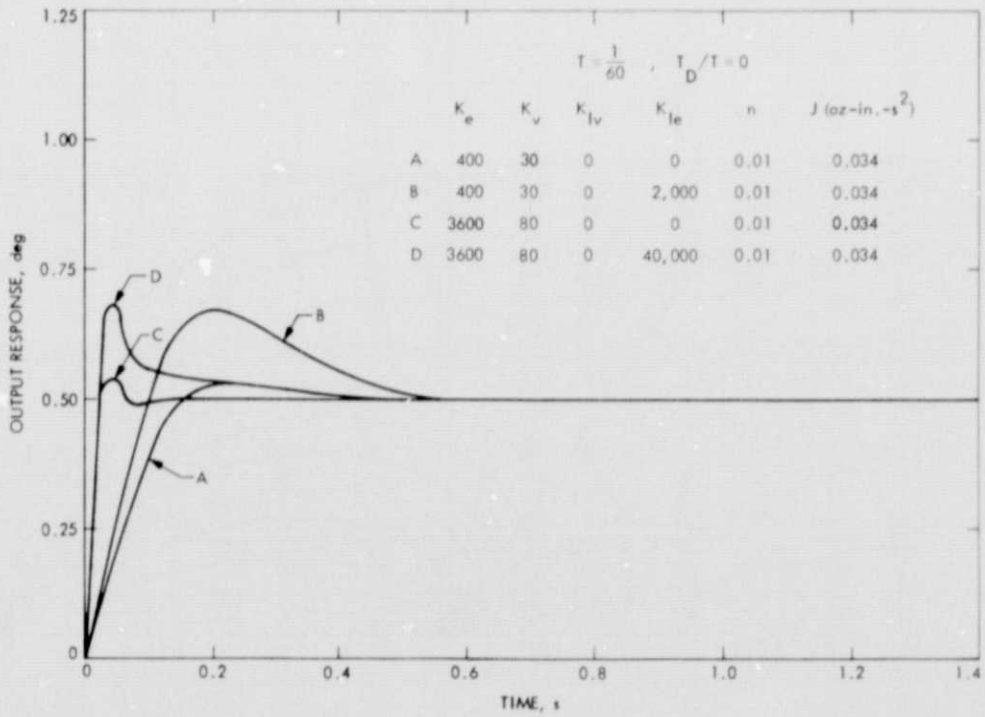

Figure A-14. Transient Response to a Step Displacement of 0.5 deg

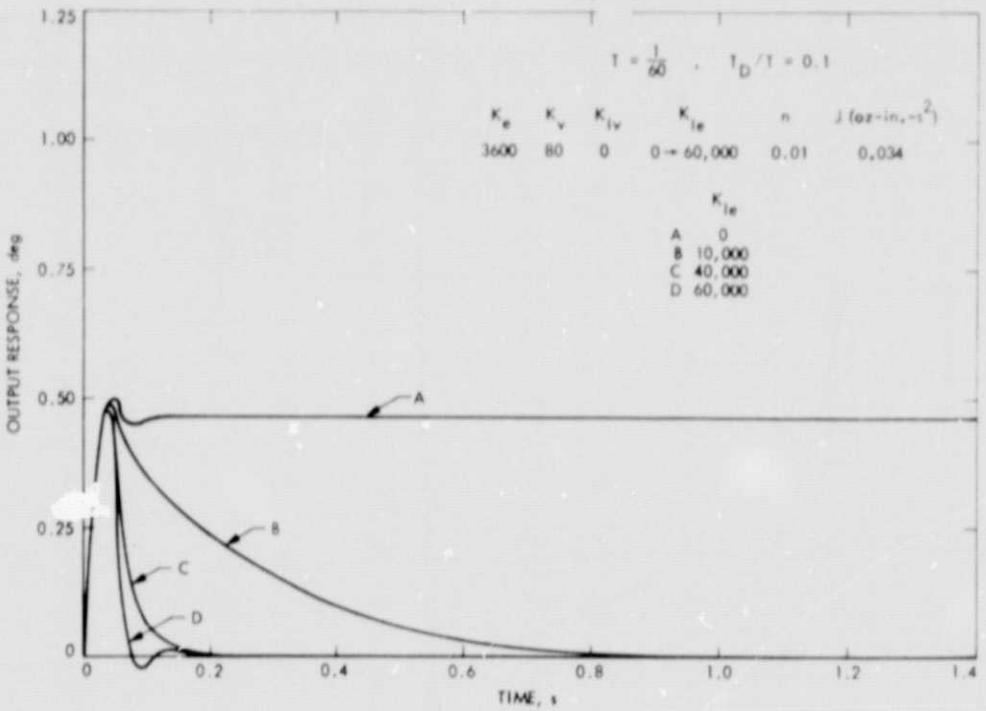

Figure A-15. Transient Response to a Step Disturbance Torque of 10,000 oz-in.

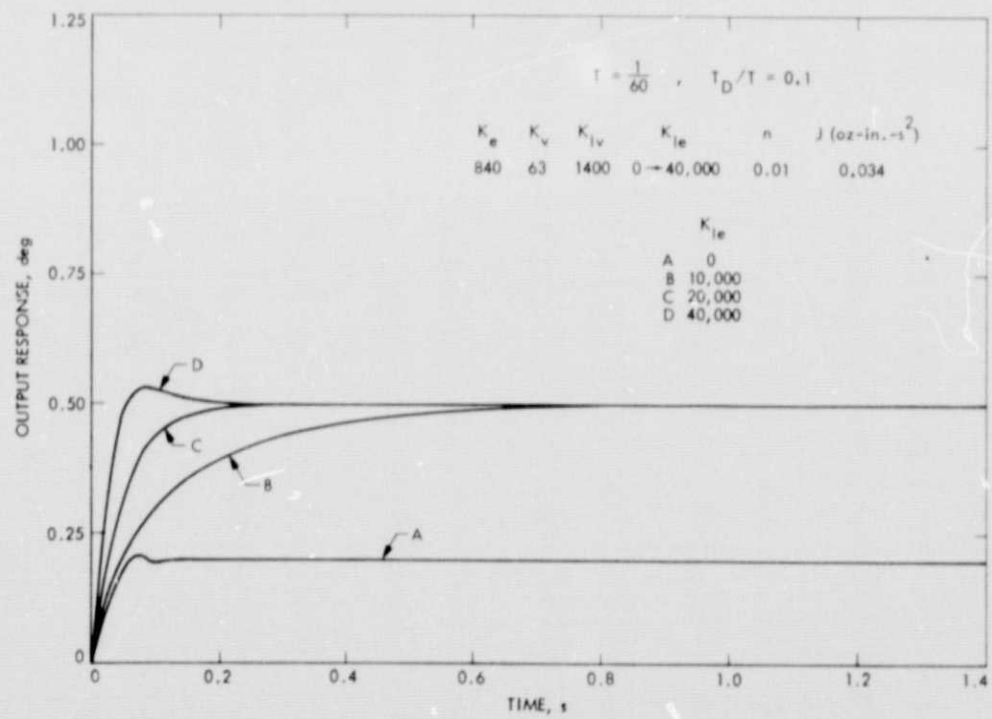

Figure A-16. Transient Response to a Step Displacement of 0.5 deg With 10% Delay

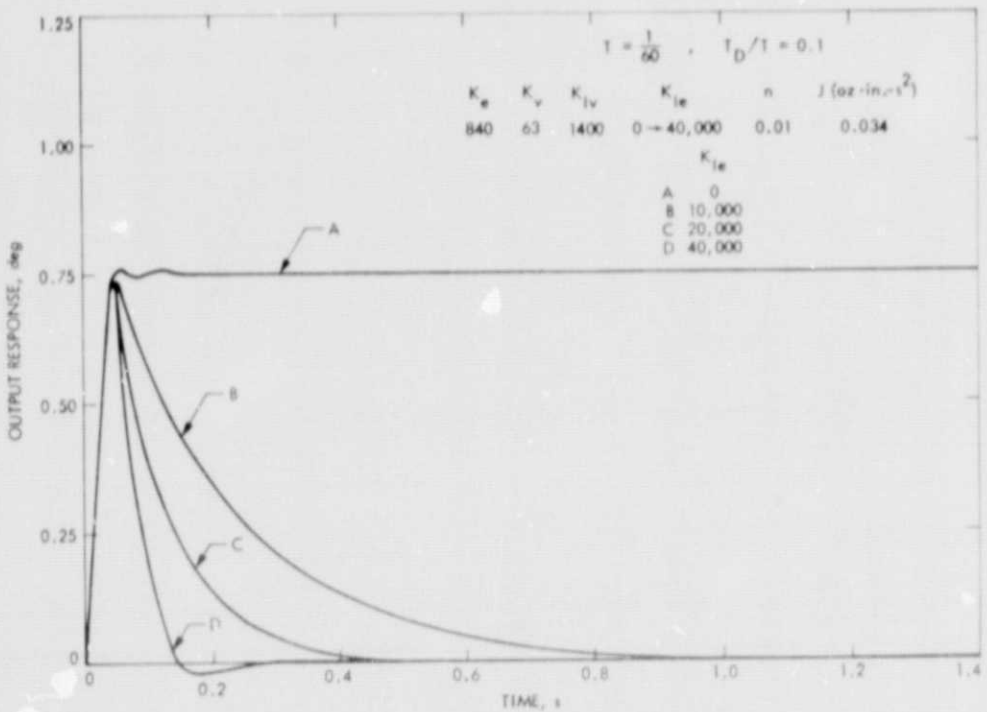

Figure A-17. Transient Response to a Step Disturbance Torque of 10,000 oz-in. With 10% Delay

NASA—JPL—Coml., L.A., Calif.